

# CALIBRATION OF HURRICANE IMAGING RADIOMETER C-BAND RECEIVERS

Sayak K. Biswas<sup>1</sup>, Daniel J. Cecil<sup>2</sup> and Mark James<sup>2</sup>

<sup>1</sup>Universities Space Research Association, Huntsville, AL 35805

<sup>2</sup>NASA Marshall Space Flight Center, Huntsville, AL 35 805

## ABSTRACT

The laboratory calibration of airborne Hurricane Imaging Radiometer's C-Band multi-frequency receivers is described here. The method used to obtain the values of receiver front-end loss, internal cold load brightness temperature and injected noise diode temperature is presented along with the expected RMS uncertainty in the final calibration.

**Index Terms**— HIRAD, Radiometer, Calibration

## 1. INTRODUCTION

Hurricane Imaging Radiometer (HIRAD) instrument uses interferometric aperture synthesis technique to create a wide-swath high resolution image of the Brightness Temperature ( $T_b$ ) distribution at four discrete C band frequencies (4, 5, 6 & 6.6 GHz) from a fixed antenna without any electrical/mechanical scanning [1]. From these  $T_b$  measurements an image of the ocean surface wind speed can be inferred. The basic measurement of an interferometric imager is the complex cross-correlation between the voltage signals from pairs of antenna separated by a distance (baseline) [2]. Usually multiple baseline measurements are required to create a  $T_b$  image. HIRAD antenna is a minimum redundancy thinned array where 36 interferometer baselines are sampled from just 10 linear antenna elements [3]. Each of the 10 antenna elements are connected to a dedicated super-heterodyne receiver which sequentially translates the Radio-Frequency (RF) passbands centered at 4, 5, 6 and 6.6 GHz to a common Intermediate Frequency (IF) band centered at 187.5 MHz by switching the Local Oscillator (LO) frequencies. Each receiver output is digitized and the complex-correlations are computed in the digital domain [4] by the Digital Back End (DBE). Each receiver has two internal calibration loads (ambient/warm and cold) and a correlated noise diode input for third calibration reference. If the noise temperatures of these internal references are known then the receiver gain and offset variation is precisely determined during flight. From which the noise temperature at the receiver input (Antenna Temperature) can be computed from the measured radiometer counts. In this paper we describe a test that was intended to determine the values of internal cold load noise

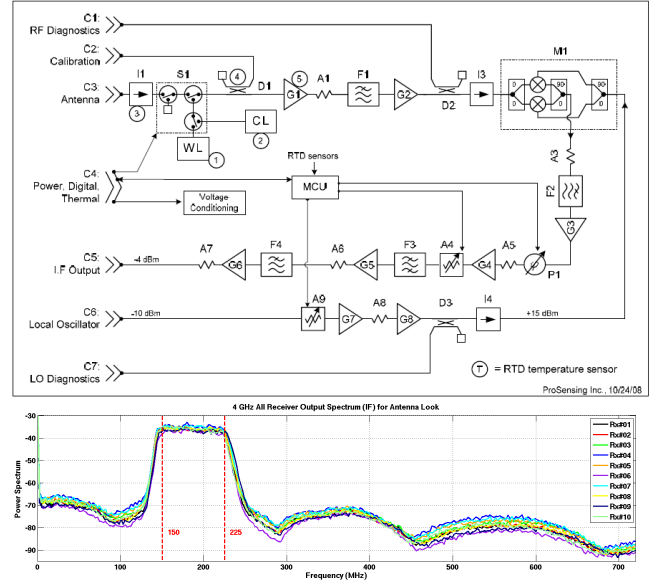


Figure 1: HIRAD receiver schematic (top) and output spectrum (bottom)

temperature ( $T_c$ ) and injected excess noise diode temperature ( $T_{ND}$ ) based upon known ambient load temperature ( $T_w$ ) and additional external inputs. However, the test data showed an apparent inconsistency with the  $T_w$ . Therefore,  $T_c$  wasn't uniquely determined, rather, a pre-determined (from the manufacturing company) value of  $T_c$  was used to determine a receiver front end loss ( $L_{fe}$ ) and  $T_{nd}$ . The method to obtain the values of  $L_{fe}$ ,  $T_c$  and  $T_{nd}$  used in current HIRAD calibration is presented here along with the expected RMS uncertainty in the calibration.

## 2. HIRAD C-BAND RECEIVER

HIRAD receivers were designed and manufactured by Prosensing Inc. [5] of Amherst, MA under a contract with the NASA Marshall Space Flight Center (MSFC) in Huntsville, AL. Fig. 1 top panel shows a schematic of the analog portion of the Prosensing receiver [6]. During normal operation the antenna output (signal to be measured) is connected to the C3 input to the receiver. The LO signal for super heterodyne operation is provided at the C6 input. The final amplified IF output signal is generated at the C5

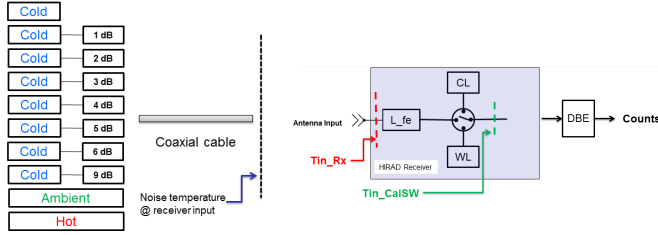


Figure 2: Test setup schematic and Simplified block-diagram for receiver front-end loss model

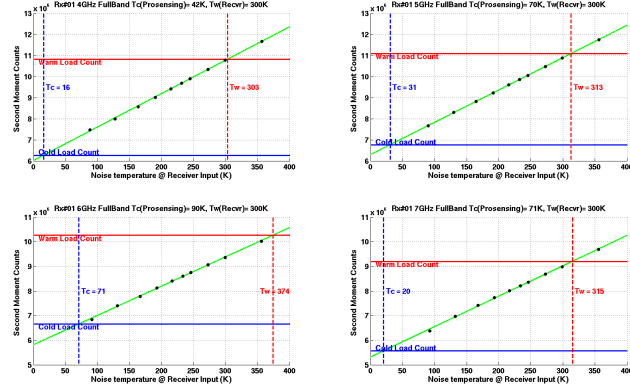


Figure 3: Average counts vs noise temperature points are plotted (black dot) for all 10 external noise inputs.

connector. The main signal path from C3 to C5 consists of an input Isolator (I1), a SP3T (Single-Pole-Triple-Throw) switch assembly, Amplification and Filter stages (G1, F1, G2), an Image-Reject Mixer (M1) followed by the final stages for IF pass band shaping (filter) and amplification. Apart from connecting to the antenna signal, the S1 switch switches the receiver input between two internal noise sources WL (warm/ambient) and CL (cold) – this enables a frequent two point calibration to compensate for the receiver gain and offset variation. A common (correlated) noise diode (ND) signal is distributed among all 10 receivers using phase matched RF cables (connected to C2) to add a known amount of noise to the S1 output via a directional coupler D1. By switching the ND on and off additional calibration points can be created for receiver gain/offset estimation and since the ND signal is correlated across all 10 receivers, an accurate estimation of cross-correlation gain can also be estimated from this scheme. Fig. 1 bottom panel shows the measured output power spectrum for all 10 receivers. The desired IF passband is only 75 MHz wide (between 150 and 225 MHz). All the receivers have the similar output spectrum shaped by the IF output filter stage. This signal is digitized at 150 MSa/s (at Nyquist rate) by the DBE for further signal processing and detection [4]

### 3. TEST DESCRIPTION

The test involved injecting precisely known noise temperature at the receiver antenna input. For this, Maury Microwave Corporation’s MT7118J Coaxial Cryogenic

Termination as the COLD reference, the MT7108B Thermal termination as the HOT reference and a custom built AMBIENT termination as a third independent reference point were used. Additional seven different noise temperature references were generated by adding 1, 2, 3, 4, 5, 6 and 9 dB coaxial attenuators respectively to the output of the COLD reference. The schematic of the test setup is shown in left hand side of Figure 2. The loss of the semi-rigid coaxial cable was measured and its temperature was monitored during the test so that its noise contribution can be estimated.

One 30 sec average count value per noise input was computed. These average counts are plotted in Figure 3 (black dots) with their corresponding  $T_{RX\_INPUT}$  (noise at the receiver input) as the abscissa. The best fit line (green) through these points represents a linear  $T_{RX\_INPUT}$  to counts transfer function. The slope of the line is the receiver system gain. The WL & CL noise temperatures ( $T_w$  &  $T_c$ ), referenced at the receiver input, could be computed from the corresponding counts using this linear equation. This procedure is shown graphically in Figure 3, where the abscissa value of the intersection of the solid red line and the solid green line gives the value of  $T_w$  and similarly the value of  $T_c$  is obtained from the intersection of the solid blue and solid green lines.

### 4. RECEIVER FRONT-END MODEL

The signal path from the output of the calibration (cal) switch S1 onwards is common among the three signals (Figure 1). Therefore to account for the radiometer count differences between Antenna, WL and CL we need to only model the differences among signal paths up to the S1 output. The SP3T switch assembly S1 consists of three SPDT (Single-Pole Double throw) switches. From the WL and CL output the noise signal has to travel through two SPDT switch losses to arrive at the cal switch output reference point. The antenna signal also pass through two switch losses; and an additional input isolator (I1) loss. If all the switches have similar loss characteristics and interconnects are designed properly then the extra loss in the antenna signal path should be equal to the insertion loss of I1. Therefore, a simplified block diagram of right hand side of Figure 2 can be assumed. The excess loss in the antenna signal path is represented by an equivalent “front-end loss” with transmission coefficient  $L_{FE}$ . Signal paths for WL and CL are assumed to be lossless. All signals travel through a lossless SP3T switch to cal switch output reference. If the noise temperature at the cal switch output be  $T_{CAL\_SWITCH}$  and that at the receiver input be  $T_{RX\_INPUT}$ , then the relation between the two is given by,

$$T_{CAL\_SWITCH} = T_{RX\_INPUT} \times L_{FE} + (1 - L_{FE}) \times T_{FE} \quad (1)$$

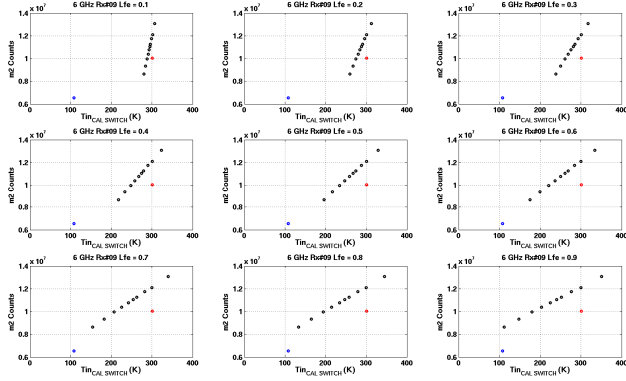


Figure 4: Effect of  $L_{FE}$  variation on  $T_{CAL\_SWITCH}$  for receiver #9 at 6 GHz

Where,  $T_{FE}$  is the physical temperature of the front end loss measured using RTD #3 (in Figure 1). Because of the assumed lossless transmission, noise temperatures due to CL & WL at the cal switch output ( $T_c$  &  $T_w$ ) are equal to those at the respective load output. To use Equation 1 for receiver calibration, the values of  $L_{FE}$  for all 10 receivers need to be known at the 4 HIRAD measurement frequencies. Information in the test data is not sufficient to solve for  $L_{FE}$ ,  $T_w$  and  $T_c$  independently. Therefore, a priori estimate of either  $T_w$  or  $T_c$  is required to solve for  $L_{FE}$ .

## 5. WARM LOAD ANCHORED CALIBRATION

WL is a passive matched RF termination and its noise temperature  $T_w$  is given by its physical temperature. Therefore  $T_w$  should be known quantity from the RTD #1 measurement. In the 2D space defined by  $\{T_{CAL\_SWITCH}, \text{count } (C)\}$ , the WL is a fixed point given by  $(T_w, C_w)$ . Here  $C_w$  is the measured WL count. The black calibration points in Figure 3 are in  $\{T_{RX\_INPUT}, C\}$  space. If these points are mapped to the  $\{T_{CAL\_SWITCH}, C\}$  space using Equation 1, then the slope and offset of the new best-fit line is going to vary depending on the value of  $L_{FE}$ . Ideally, if there exists a value of  $L_{FE}$  for which the new best-fit line through these cal points in the  $\{T_{CAL\_SWITCH}, C\}$  space also passes through the point  $(T_w, C_w)$ , then that will be the desired solution for  $L_{FE}$ . Practically, the value of  $L_{FE}$  for which the residual error of the linear fit through all the cal points and the WL point is the minimum is the solution.

Figure 4 demonstrates the effect of  $L_{FE}$  on the cal points (black circles) in the  $\{T_{CAL\_SWITCH}, C\}$  space for receiver #9 at 6 GHz. Each subpanel is a plot for a different  $L_{FE}$  value. The red circle is the fixed WL point ( $T_w, C_w$ ) which doesn't depend on  $L_{FE}$ . It should be noted that the red point tends to align with the black ones only for a very small value of  $L_{FE}$  ( $\sim 0.1$ ). A small value of transmission coefficient ( $L_{FE}$ ) indicates very high loss. The expected value of  $L_{FE}$  is between 0.88 – 0.96 from the isolator loss measurements done by Prosensing. Therefore a value of 0.1 is far from being reasonable. The residual error (of the line

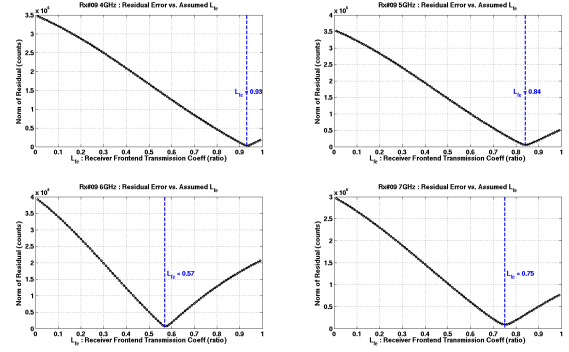


Figure 5: Residual error of the best linear fit through the calibration & cold load points for various values of  $L_{FE}$

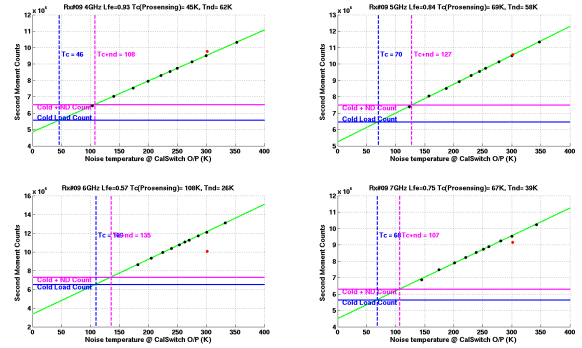


Figure 6: Final  $T_{CAL\_SWITCH}$  to  $C$  transfer function and estimated  $T_{ND}$  values for Receiver #9

fit) vs  $L_{FE}$  for all 4 frequencies are computed for all 10 receivers derived from the warm load anchored calibration. None of them provided a reasonable solution for  $L_{FE}$ . Therefore, instead of the WL point, a new calibration based on the CL was attempted next.

## 6. COLD LOAD ANCHORED CALIBRATION

### 6.1. Determination of front-end loss ( $L_{FE}$ )

For cold load anchored calibration the  $T_c$  values measured by Prosensing are assumed to be true. Since these  $T_c$  values are referenced at the CL output, according to the assumed model described in Figure 2, they should be the same at the output of the lossless SP3T switch. Therefore the CL point,  $(T_c, C_c)$ , is a fixed point in the  $\{T_{CAL\_SWITCH}, C\}$  space which doesn't depend on  $L_{FE}$ . This point is represented by the blue circle in Figure 4. It should be noted that for the value of  $L_{FE} = 0.6$  the CL point seems to line up with the external cal points (black circles). For  $L_{FE}$  values less than or greater than 0.6 the line defined by the cal points moves away from the CL point. Clearly a  $L_{FE}$  solution is possible for which the residual error of the linear fit through the cal points and the CL point is the minimum. Figure 5 shows the residual error vs  $L_{FE}$  plots for receiver #9 at all 4 frequencies. Each frequency has a clearly defined minimum

Table I: Derived  $L_{FE}$ ,  $T_c$  and  $T_{ND}$  values

Receiver#	$L_{FE}$ (ratio)				$T_c$ (K)				$T_{ND}$ (K)			
	4 GHz	5 GHz	6 GHz	6.6 GHz	4 GHz	5 GHz	6 GHz	6.6 GHz	4 GHz	5 GHz	6 GHz	6.6 GHz
01	0.91	0.85	0.92	0.82	41	71	89	71	58	55	55	40
02	0.92	0.85	0.82	0.81	33	73	84	54	59	54	48	40
03	0.92	0.87	0.83	0.78	38	72	91	75	56	54	43	35
04	0.89	0.85	0.92	0.79	53	70	81	83	66	59	59	42
05	0.93	0.84	0.8	0.78	59	86	70	73	67	63	44	42
06	0.8	0.78	0.79	0.75	79	93	80	88	49	50	39	36
07	0.92	0.88	0.78	0.82	50	60	84	68	69	64	44	45
08	0.9	0.83	0.74	0.79	52	64	81	103	60	55	38	43
09	0.93	0.84	0.57	0.75	46	70	109	68	62	58	26	39
10	0.81	0.74	0.76	0.71	75	88	132	104	53	50	47	44

error point and the corresponding  $L_{FE}$  solutions are noted in the figure. The  $L_{FE}$  solution at 6 GHz for receiver #9 indicates much higher front-end loss than expected. The behavior of receiver #9 at 6 GHz is very different from the other receiver- frequency combinations. In other words, most of our assumptions to define the simplistic front-end model (Figure 2) are probably violated in receiver #9 at 6 GHz. Therefore the computed  $L_{FE}$  value in this case is probably far from the true representative of the front-end loss. However, all other receiver-frequency combinations yielded acceptable  $L_{FE}$  values (Table I). In general, there is a monotonic increase in the loss value from 4 to 6.6 GHz (i.e. decrease in the transmission coefficient,  $L_{FE}$ ) for all 10 receivers. This characteristic is consistent with the physical behavior of a loss in general.

## 6.2. Determination of noise diode temperature ( $T_{ND}$ )

To determine the two unknown receiver parameters (gain and offset), two independent internal calibration noise references are required. For this reason WL and CL are included in the receiver hardware. However, WL cannot be used as the corresponding test data is not consistent with the assumed calibration model. Therefore the CL + Noise Diode (ND) signal is used for determination of gain and offset terms. Figure 6 shows the determination of this additional noise temperature added by the noise diode ( $T_{ND}$ ) graphically. The best-fit line for the  $T_c$  anchored calibration in the  $\{T_{CAL\_SWITCH}, C\}$  space is shown in green. The minimum residual error  $L_{FE}$  values derived in section 6.1 are used to derive the  $T_{CAL\_SWITCH}$  values for the external calibration load points (black dots). The  $L_{FE}$  and the Prosensing  $T_c$  values are given in the figure titles. The abscissa values of the intersections of this line with the CL counts level (blue) and the CL+ND counts level (magenta) are the solutions for  $T_c$  and  $T_c+T_{ND}$ . Where  $T_c+T_{ND}$  is the noise temperature looking at the CL with the noise diode turned on.  $T_{ND}$  is the difference between  $T_c+T_{ND}$  and  $T_c$ . The WL point in red is shown in the Figure 6 just for a comparison. The way it is positioned far from the green line at 6 GHz indicates some issue with the receiver hardware which needs to be addressed in any possible future receiver development effort. Derived  $T_{ND}$  values for all 10 receivers are given in Table I.

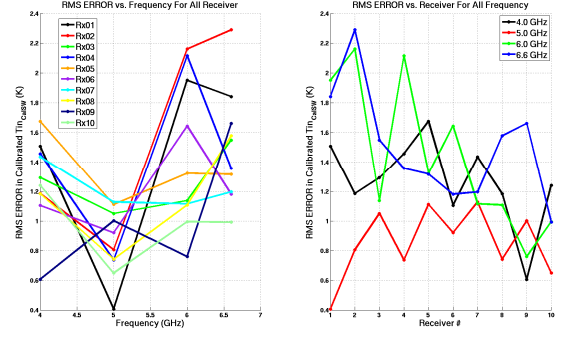


Figure7: The RMS uncertainties in the calibrated  $T_{CAL\_SWITCH}$

The uncertainty in the calibration of  $T_{CAL\_SWITCH}$  is the horizontal distance between the external reference calibration points (black) and the green best-fit line in Fig. 6. The root mean squared (RMS) value of these differences for all the cal points, including the Prosensing cold load point, is the estimated RMS calibration uncertainty at the cal switch output. The RMS error vs frequency is plotted for all 10 receivers in the left panel of Fig. 7. The right hand panel of the figure shows the same plotted against Receiver #. It appears that the 5GHz channel has the lowest error across all receivers. Overall, the RMS uncertainty varies from 0.4 – 2.3 K across all receiver, frequency combinations.

## 7. CONCLUSION

The laboratory calibration of HIRAD receivers is described here. The method used to obtain the values of receiver front-end loss, internal cold load brightness temperature and injected noise diode temperature is presented. Warm load was excluded from the calibration due to an anomaly. The final RMS uncertainty in calibration is 0.4-2.3 K at the cal switch output.

## 11. REFERENCES

- [1] C. Ruf *et al.*, "The hurricane imaging radiometer - an octave bandwidth synthetic thinned array radiometer," *IGARSS 2007. IEEE International*, Barcelona, 2007, pp. 231-234.
- [2] C. Ruf, J. B. Roberts, S. Biswas, M. James and T. Miller, "Calibration and image reconstruction for The Hurricane Imaging Radiometer (HIRAD)," *IGARSS, 2012 Munich*, pp. 4641-4643.
- [3] M. C. Bailey *et al.*, "Multi-Frequency Synthetic Thinned Array Antenna for the Hurricane Imaging Radiometer," in *IEEE Transactions on Antennas and Propagation*, vol. 58, no. 8, pp. 2562-2570, Aug. 2010.
- [4] "HIRAD 10 Channel Correlator Subsystem Functional Specification", Revision X12, 01 Oct, 2014.
- [5] <http://prosenensing.com/>
- [6] "CCR2008-C HIRAD C-Band Receiver Interface manual", Revision E; June 18, 2009, Prosensing Inc.